Solvent/Non-solvent Sintering: A Novel Route to Create Porous Microsphere Scaffolds for Tissue Regeneration

Justin L. Brown,[1] Lakshmi S. Nair,[2] Cato T. Laurencin[1,2,3]

[1] Department of Biomedical Engineering, University of Virginia, Virginia

[2] Department of Orthopaedic Surgery, University of Virginia, Virginia

[3] Department of Chemical Engineering, University of Virginia, Virginia

Received 23 July 2007; revised 3 October 2007; accepted 24 October 2007
Published online 27 December 2007 in Wiley InterScience (www.interscience.wiley.com). DOI: 10.1002/jbm.b.31033

Abstract: Solvent/non-solvent sintering creates porous polymeric microsphere scaffolds suitable for tissue engineering purposes with control over the resulting porosity, average pore diameter, and mechanical properties. Five different biodegradable biocompatible polyphosphazenes exhibiting glass transition temperatures from −8 to 41°C and poly (lactide-*co*-glycolide), (PLAGA) a degradable polymer used in a number of biomedical settings, were examined to study the versatility of the process and benchmark the process to heat sintering. Parameters such as: solvent/non-solvent sintering solution composition and submersion time effect the sintering process. PLAGA microsphere scaffolds fabricated with solvent/non-solvent sintering exhibited an interconnected porosity and pore size of 31.9% and 179.1 μm, respectively which was analogous to that of conventional heat sintered PLAGA microsphere scaffolds. Biodegradable polyphosphazene microsphere scaffolds exhibited a maximum interconnected porosity of 37.6% and a maximum compressive modulus of 94.3 MPa. Solvent/non-solvent sintering is an effective strategy for sintering polymeric microspheres, with a broad spectrum of glass transition temperatures, under ambient conditions making it an excellent fabrication route for developing tissue engineering scaffolds and drug delivery vehicles. © 2007 Wiley Periodicals, Inc. J Biomed Mater Res Part B: Appl Biomater 86B: 396–406, 2008

Keywords: polyphosphazene; sintered microspheres; poly(lactide-*co*-glycolide); scaffolds; tissue engineering

INTRODUCTION

Three-dimensional porous scaffolds are a crucial aspect of scaffold-based tissue engineering as they allow for the adhesion and proliferation of cells and assist the three dimensional organization of cells during tissue regeneration. In addition, the scaffolds should be able to provide appropriate mechanical support to the repairing tissue. Our laboratory made one of the first attempts to develop porous structures having mechanical properties in the range of trabecular bone as scaffolds for bone tissue engineering.[1–3] The scaffolds were developed from sintered poly(lactide-*co*-glycolide), (PLAGA), microspheres. PLAGA is an FDA approved biodegradable polymer that undergoes hydrolysis resulting in lactic acid and glycolic acid.[4] The sintered PLAGA microsphere scaffolds were fabricated by placing PLAGA microspheres into a mold and then heating the mold to a point just beyond the glass transition temperature of the polymeric microspheres.[1–3,5–7] In doing so the microspheres were sintered into a porous scaffold with an interconnected pore structure. It has been found that the pore size and pore volume of the scaffolds can be varied by changing the duration/temperature of sintering as well as the initial diameter of the microspheres.[1,5,8,9] The resulting porous structures were found to be highly osteoconductive and human osteoblast cells were able to maintain phenotype during *in vitro* culture on the scaffolds.[2,5,8,9] *In vivo* studies using a critical size defect in a rabbit model made evident that scaffolds are capable of regenerating bone *in vivo*.[7]

Using heat to sinter PLAGA microspheres is an effective method for creating PLAGA microsphere scaffolds, however; heat sintering is not applicable across a broad

Correspondence to: C. T. Laurencin (e-mail: laurencin@virginia.edu)
Contract grant sponsor: NIH; Contract grant numbers: R01 AR052536, R01 EB004051
Contract grant sponsor: NSF; Contract grant number: BES-0503207
Contract grant sponsor: USArmy; Contract grant number: W81XWH-07-1-050579

© 2007 Wiley Periodicals, Inc.

spectrum of polymer types due to its dependence on specific physicochemical properties, such as: glass transition temperature, specific heat, crystallinity, viscosity, and surface tension of the polymer to be sintered.[10] This specific criteria for sintering of polymers, such as polyphosphazenes, limits the applicability of heat sintering.

Polyphosphazenes are inorganic–organic macromolecules with an inorganic phosphorous–nitrogen backbone and two organic side groups attached to each phosphorous atom.[11] Because of the high flexibility of the P–N backbone, the properties of the polyphosphazenes depend on the side group chemistry. Therefore, by varying the side groups, different classes of polyphosphazenes having a wide spectrum of properties can be synthesized.[11–13] Among these, amino acid ester polyphosphazenes having different amino acid ester side groups have been found to be biodegradable and biocompatible. Our laboratory has demonstrated the excellent osteocompatibility of biodegradable amino acid ester polyphosphazenes using *in vitro* and *in vivo* models.[13,14] Additionally, amino acid ester polyphosphazenes degrade into neutral and nontoxic by-products consisting of the corresponding amino acid, an alcohol derived from the ester, and an ammonium phosphate buffer solution.[11,12] These properties make amino acid ester substituted biodegradable polyphosphazenes a promising biomaterial, and efforts are ongoing to develop three-dimensional porous structures from biodegradable polyphosphazenes for bone tissue engineering applications.[13–16]

The objective of this study was to develop a novel and versatile method of sintering polymeric microspheres under ambient conditions using partial dissolution of the microsphere surface, based on Flory–Huggins solution theory, to form porous three dimensional structures for tissue engineering applications. Flory–Huggins solution theory deals with the interplay between monomer:monomer and monomer:solvent interaction in a polymer:solvent mixture.[17] Our aim was to use these interactions to create a solvent/non-solvent mixture that establishes a balance between polymer dissolution and precipitation. During this intermediate state the microsphere surfaces were susceptible to bonding with adjacent microspheres prior to precipitation of the intertwined surface chains and sintering of the microspheres. This sintering method was benchmarked with solvent/non-solvent sintered PLAGA microspheres compared with heat sintered PLAGA microspheres and the flexibility tested by applying the technique across a spectrum of five polyphosphazenes having glass transition temperatures varying from -8 to 41°C. Additionally the sintering method was used to develop lighter than water amino acid ester substituted polyphosphazene microsphere scaffolds for bioreactor based tissue engineering. The morphology and pore structure of the PLAGA solvent/non-solvent sintered scaffolds was compared with that of PLAGA heat sintered microsphere scaffolds. The morphology, porosity and mechanical properties of the three amino acid ester substituted polyphosphazene microsphere scaffolds composed of mixed solid and hollow microspheres were evaluated for desirable properties of a microsphere scaffold for use in bioreactor based bone tissue engineering as well as drug delivery applications.

MATERIALS AND METHODS

Polyphosphazene Synthesis

All polyphosphazenes were synthesized as reported previously.[11,18,19] Briefly, purified hexachlorotriphosphazene (Nippon Fine Chemicals, Japan) was polymerized to polydichlorophosphazene by a ring opening polymerization in a sealed tube at 250°C. The chlorine side groups of the polydichlorophosphazene were then substituted with one or a combination of alanine ethyl ester hydrochloride, valine methyl ester hydrochloride, phenylalanine ethyl ester hydrochloride, p-cresol, and phenyl phenol (Sigma-Aldrich, St. Louis, MO) as reported previously.[11,18,19] The substituted polymer was then precipitated out in hexane (Sigma-Aldrich, St. Louis MO) to form either poly[bis(ethyl alaninato)phosphazene], PNEA, poly[bis(methyl valinato)phosphazene], PNMV, poly[bis(ethyl phenylalaninato) phosphazene], PNEPhA, poly[(ethyl alaninato)$_1$(methyl phenoxy)$_1$ phosphazene], PNEAMPh, or poly[(ethyl alaninato)$_1$(phenyl phenoxy)$_1$ phosphazene], PNEAPhPh. The completion of the substitution reaction was followed by ^{31}P NMR. The fabricated polymers were characterized by their molecular weigh using an 1100 Series GPC (Hewlett Packard, Palo Alto, CA), chemical structure with ^{1}H and ^{31}P NMR using a UnityInova 300/54 (Varian, Palo Alto, CA), and glass transition using Q1000 differential scanning calorimeter (TA Instruments, New Castle, DE).

Microsphere Fabrication

PLAGA composed of 50:50 lactide:glycolide, (Lakeshore Biomaterials, Birmingham, AL) was dissolved in methylene chloride (Sigma-Aldrich, St. Louis, MO) and poured into a stirred solution of poly(vinyl alcohol), PVA, (Sigma-Aldrich, St. Louis, MO) as described previously.[2,8] The microspheres were then isolated using vacuum filtration, washed twice with deionized water and allowed to air dry for several hours. The microspheres were then lyophilized for an additional 48 h to ensure total solvent removal, and sieved into various size ranges.

Solid PNEA, PNMV, and PNEPhA microspheres were made following similar methods to the PLAGA microspheres by using the water/oil emulsion technique coupled with solvent evaporation. The PNEA was dissolved in methylene chloride at 5% (wt/vol), the PNMV was dissolved in methylene chloride at 35% (wt/vol) and the PNEPhA was dissolved in methylene chloride at 25% (wt/vol). Each solution was slowly poured into a solution of 1% (wt/vol) PVA stirred at 360 rpm. Additionally, porous PNEA, PNMV and PNEPhA microspheres were fabricated for future *in vitro* bioreactor studies. The porous microspheres were fabricated by a triple emulsion technique through the

addition of 10% (vol/vol) water and 10% (vol/vol) hexane to the dissolved polymer. The resulting double emulsion was poured as before into a stirred solution of PVA. After solvent evaporation the microspheres were collected by vacuum filtration and lyophilized and sieved to harvest microspheres with diameters in the 355–425 μm range.

PNEAMPh and PNEAPhPh microspheres were made by dissolving each in methylene chloride at 7% (wt/vol), and poured slowly into a solution of 1% (wt/vol) PVA. The microspheres were then collected by vacuum filtration, lyophilized, but were not sieved as they were to be used solely as a proof of concept.

Microsphere Sintering

For each polymer, a solvent and non-solvent were selected such that the solvent was more volatile than the non-solvent and the two were miscible with each other. For the PLAGA microspheres the selected solvent was acetone and the selected non-solvent was ethanol (Sigma-Aldrich, St. Louis, MO), for the PNEA, PNEAMPh, and PNEAPhPh the selected solvent was acetone (Sigma-Aldrich, St. Louis, MO) and the selected non-solvent was hexane, for the PNMV and PNEPhA the selected solvent was THF (Sigma-Aldrich, St. Louis, MO) and the selected non-solvent was again hexane. Each solvent was combined with the corresponding non-solvent from 1 to 50% of the total volume being solvent. Approximately 50 mg of each polymeric microsphere were placed in a glass vial, with one glass vial for each solvent/non-solvent concentration. Then $\sim$200 μL of solvent/non-solvent sintering solution was pipetted over the microspheres to create a heterogeneous mixture. Each vial was vortexed for $\sim$5 s to ensure thorough wetting of the microspheres surface. The wetted microspheres were then transferred to a cylindrical mold 4 mm in diameter and 2.5 mm in length. The solvent/non-solvent sintering solution was allowed to evaporate from the molded microspheres for 30 min under a fume hood before being placed under vacuum for an additional 24 h to ensure total removal of the solvent/non-solvent sintering solution.

Porosimetry and mechanical compression testing was performed on PNEA, PNMV, and PNEPhA scaffolds sintered with a high, medium, and low solvent/non-solvent sintering solution and containing a blend of solid and porous microspheres to create a scaffold with a final density less than water. For these quantitative measurements the following solvent/non-solvent sintering solutions will be used: PNEA microspheres sintered with 17.5% (low), 20% (mid), and 22.5% (high) (vol/vol) acetone/hexane solutions, PNMV microspheres sintered with 12.5% (low), 15% (mid), and 17.5% (high) (vol/vol) THF/hexane solutions and PNEPhA microspheres sintered with 30% (low), 32.5% (mid), and 35% (high) (vol/vol) THF/hexane solutions.

An additional set of experiments was performed on the PLAGA microspheres to test the effect of time on the final sintered scaffold morphology. This was accomplished by placing 50 mg of PLAGA microspheres in vials, then 200 μL of 20% (vol/vol) acetone/ethanol sintering solution was added to each vial, the vials were capped and they were vortexed for 5 s. After a set period of submersion time of either: 0, 1, 5, 10, or 30 min, the microspheres were transferred to the previously mentioned mold and again allowed to air dry for 30 min followed by being placed under vacuum for 24 h. After the scaffolds dried under vacuum for 24 h they were demolded with a small metal plunger designed to match the dimensions of the mold.

Scanning Electron Microscopy

Scanning electron microscope images were acquired at each concentration/time point for the PLAGA scaffolds as well as for each of the additional polymer types. An initial broad range of solvent/non-solvent ratios were used to establish a lower bound for the solvent/non-solvent sintering solution. This lower bound is defined as the minimum solvent concentration at which the scaffold can successfully be demolded. The maximum solvent/non-solvent sintering solution is defined as the composition at which the solvent/non-solvent sintering solution dissolves the polymer. All scaffolds were imaged on a JXA 840A Scanning Electron Microscope (JEOL, Tokyo, Japan) after sputter coating with gold palladium using a Hummer Sputter Coater (Anatech, Hayward, CA).

Porosity

PLAGA, PNEA, PNMV, and PNEPhA scaffolds were quantitatively characterized by porosimetry using an Autopore III mercury intrusion porosimeter (Micromeritics, Norcross, GA) to determine the interconnected porosity. PLAGA microspheres sieved into the size range of 500–600 μm and sintered with a 20% (vol/vol) acetone/ethanol solution were used to compare the solvent/non-solvent sintering method with porosities previously reported for heat sintered PLAGA microsphere scaffolds. PNEA, PNMV, and PNEPhA were sintered with low, mid, and high solvent/non-solvent sintering solutions and the porosity was measured for each. For the porosimetry a 4 mm diameter and 8 mm height mold was used, four scaffolds were used per run with a total of three runs, $n = 3$. The PNEA, PNEPhA, and PNMV scaffold porosities were compared using a one-way ANOVA with Tukey test. The method of molding and demolding the microspheres is the same as aforementioned.

Compression Testing

PNMV and PNEPhA scaffolds having the same 4 mm diameter and 8 mm height as used in the porosimetry testing were also compression tested using a uniaxial compression testing machine (Instron, Canton, MA) at a crosshead speed of 10 mm/min. PNEA, PNEAMPh, and PNEAPhPh were excluded from compression testing due to the plastic

nature of the polymers at room temperature. For each polymer type tested the same high, mid and low sintering solution concentrations were used as aforementioned. Six scaffolds, $n = 6$, of each type were used and compared using a one-way ANOVA with Tukey test.

Glass Transition Measurement

The glass transition point was obtained for PNEA, PNMV, and PNEPhA using a Q1000 differential scanning calorimeter (TA Instruments, New Castle, DE). The polymer samples were heated from −70 to 150°C at a rate of −3°C/min under a nitrogen atmosphere and the glass transition point was defined as the point of inflection on the heat capacity change thermogram.

RESULTS

Versatility of the Solvent/Non-solvent Sintering Process

A range of polymers were selected to study the versatility of the process and these three polymers are summarized in Table I, which provides information regarding the chemical structure and glass transition temperature for the five different polymers used to study the versatility of the solvent/non-solvent sintering process. The polymers selected illustrated a range of glass transition temperatures from −7.63 to 40.72°C.

The versatility of solvent/non-solvent sintering is illustrated in Figure 1, which shows the SEMs of PLAGA, PNEA, PNEAPhA, PNEAMPh, and PNEAPhPh polymeric microspheres sintered together by the solvent/non-solvent process. For each polymer type a solvent system was selected based on the following parameters: the solvent is more volatile (higher vapor pressure at room temperature and pressure) than the non-solvent, the solvent and non-solvent are miscible, and there exists no azeotropes across the range of solvent/non-solvent ratios. Figure 1(A). shows PLAGA sintered with a 20% (vol/vol) acetone/ethanol solution. Figure 1(B) illustrates PNEA microspheres sintered with a 40% (vol/vol) acetone/hexane solution. Figure 1(C) illustrates PNEPhA microspheres sintered with a 30% (vol/vol) THF/hexane solution. Figure 1(D) illustrates PNMV microspheres sintered with a 15% (vol/vol) THF/hexane solution. Figure 1(E,F) illustrates PNEAPhPh and PNEAMPh sintered with a 15% (vol/vol) acetone/hexane solution. As evidenced from the figures all the polymeric microspheres are effectively sintered together without any significant changes in the spherical morphology of the microspheres. The sintered structure exhibited interconnected pores with no signs of polymer dissolution and filling the pores between the microspheres.

Effect of Solvent Concentration on Sintering

The effect of solvent concentration was studied and the results are shown in Figure 2, which depicts the effect of

TABLE I. Depiction of Polymer Structure and Glass Transition Temperature

Polymer	Structure	T_g
PLAGA	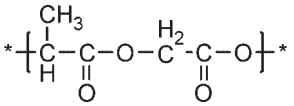	35.7°C[20]
PNEA	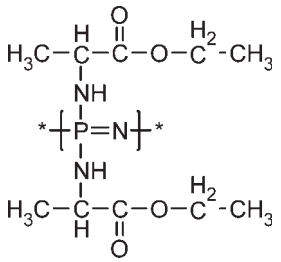	−7.63°C
PNMV	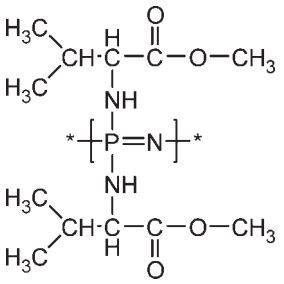	37.21°C
PNEPhA	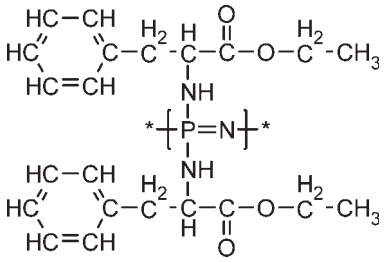	40.72°C
PNEAMPh	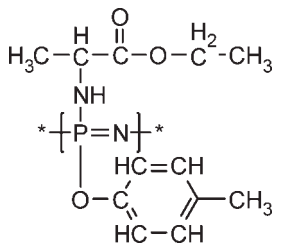	−6°C[13]
PNEAPhPh	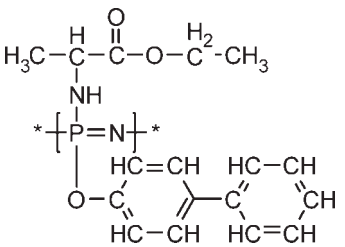	18°C[13]

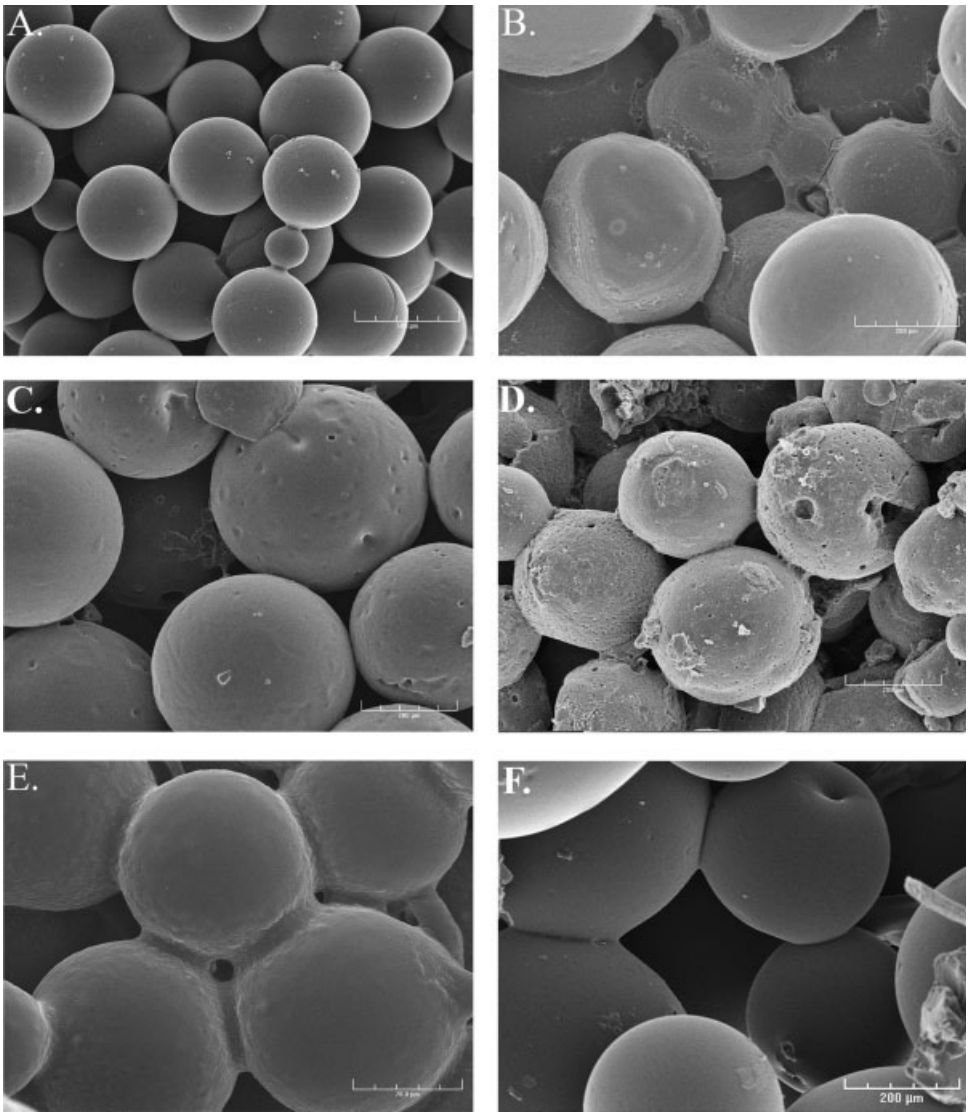

Figure 1. SEM images illustrating the flexibility of solvent/non-solvent sintering on creating porous sintered microsphere scaffolds from a wide array of different polymer types. A. PLAGA, B. PNEA, C. PNEPhA, D. PNMV, E. PNEAPhPh, F. PNEAMPh.

the concentration of the sintering solution on the degree of sintering between the microspheres. For each concentration there is a low magnification image taken at 50× as well as a high magnification image taken at 100×, excluding 10 and 15% (vol/vol) acetone/ethanol solvent composition as there was no discernible visual difference between these two concentrations and the 20% (vol/vol) acetone/ethanol solvent composition. The PLAGA microspheres sintered at concentrations less than 10% (vol/vol) acetone/ethanol did not survive demolding and were discarded from the analysis. The scaffolds sintered with the 10% (vol/vol) acetone/ethanol solvent composition remained intact after demolding suggesting that the microspheres were indeed sintered even though it is difficult to see the region where the microspheres are joined together. As the concentration increases from 10% (vol/vol) acetone/ethanol the bonding region between the microspheres becomes more evident. At a concentration of 40% (vol/vol) acetone/ethanol the sintering causes occlusion of the open porosity visible at lower concentrations. Figure 3 is a Teas graph representing the fractional solubility parameters (f_d for the dispersion force, f_p for the polar force, f_h for the hydrogen bonding force) for common PLAGA solvents.[21,22] This allows for a representation of the solubility range of PLAGA, illustrated by the circles on the graph which each represent a PLAGA solvent. Additionally, ethanol and the 40% (vol/vol) acetone/ethanol solvent composition are represented in Figure 3 by an asterisk and a triangle respectively. It can be seen that the 40% (vol/vol) acetone/ethanol solvent composition is near to the solubility range of PLAGA before the evaporation of acetone, due to the higher vapor pressure of acetone compared with ethanol, pushes the solvent/non-solvent system away from the solubility range of PLAGA causing precipitation of dissolved polymer chains.

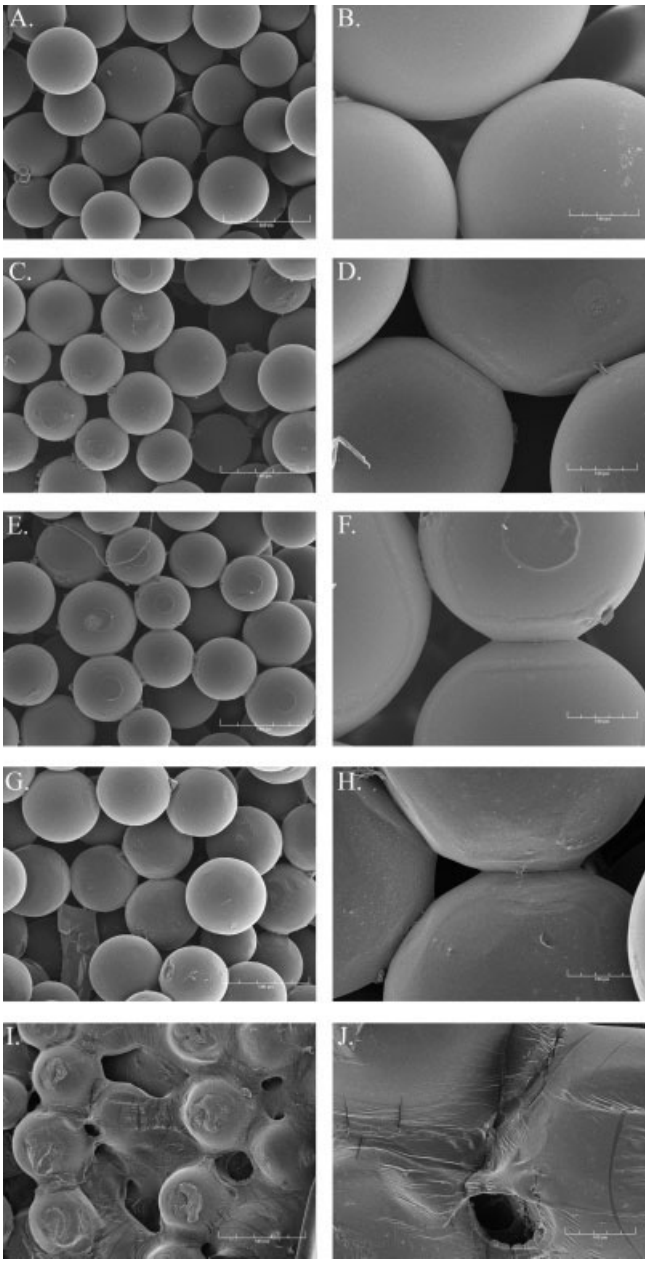

Figure 2. Effect of solvent:non-solvent ratio on the resulting morphology of the sintered microsphere scaffold. Higher solvent concentrations led to greater bonding regions between microspheres. The 50× and 200× SEM images of PLAGA scaffolds with varying acetone/ethanol sintering solution concentrations: A. 20% (vol/vol) 50×, B. 20% (vol/vol) 200×, C. 25% (vol/vol) 50×, D. 25% (vol/vol) 200×, E. 30% (vol/vol) 50×, F. 30% (vol/vol) 200×, G. 35% (vol/vol) 50×, H. 35% (vol/vol) 200×, I. 40% (vol/vol) 50×, J. 40% (vol/vol) 200×.

Effect of Time on Degree of Sintering

A study was performed by using the 20% (vol/vol) acetone/ethanol solvent/non-solvent sintering solution and varying the submersion time (0, 1, 5, 10, and 30 min) (Figure 4). PLAGA microspheres were submerged in the solution before being molded and allowing the solvent/non-solvent solution to evaporate. The region of microsphere bonding increases to a small degree with an increase in submersion time from 1 to 5 min, and increases again in small increments when the submersion times are increased from 5 to 30 min. However, the 10 and 30 min submersion times do illustrate the microspheres beginning to deform.

Scaffold Porosity

The PLAGA scaffolds sintered with 20% (vol/vol) acetone/ethanol show a total porosity of 31.9% ± 0.4% and a median pore size of 179.1 ± 2.0 μm, both of which are similar to values reported earlier for optimized heat sintered PLAGA microsphere scaffolds.[1,2] The pore distribution is represented by Figure 5 and illustrates a narrow band of pore sizes stretching from ~100 to 300 μm.

The polyphosphazene scaffolds illustrated a trend between the concentration of the sintering solution and the resulting porosity and pore size. Figures 6 and 7 depict the relationship between sintering solution concentration and the porosity and pore size respectively. From Figure 6 both the PNEA and PNEPhA microsphere scaffolds illustrate a trend of decreasing total porosity as the concentration increases. PNEA scaffold porosity is found to be 36.1% ± 1.2% for the low sintering solution, 34.6% ± 2.3% for the mid sintering solution and 27.1% ± 5.7% for the high sintering solution. PNEPhA scaffold porosity is found to be 30.9% ± 4.3% for the low sintering solution, 33.2% ± 0.8% for the mid sintering solution and 27.5% ± 2.4% for the high sintering solution. The PNEPhA scaffolds were found to have a significant decrease in porosity between the mid concentration and the high concentration. Figure 8

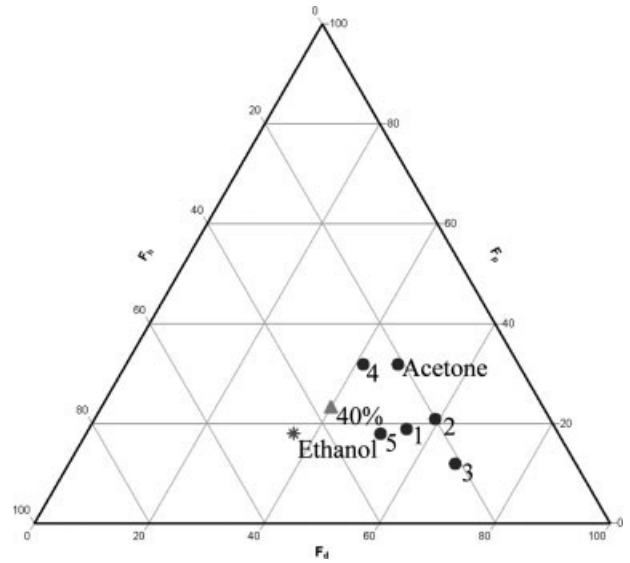

Figure 3. Teas graph illustrating solubility parameters for common PLAGA solvents that were used to select the solvent and non-solvent for solvent/non-solvent sintering of PLAGA microspheres: 1. Tetrahydrofuran, 2. Methylenechloride, 3. Chloroform, 4. *N,N* Dimethylformamide, 5. Ethylacetate. In addition Acetone a PLAGA solvent, Ethanol a PLAGA non-solvent, and the dynamic solvent/non-solvent mixture of 40% acetone/ethanol are labeled.

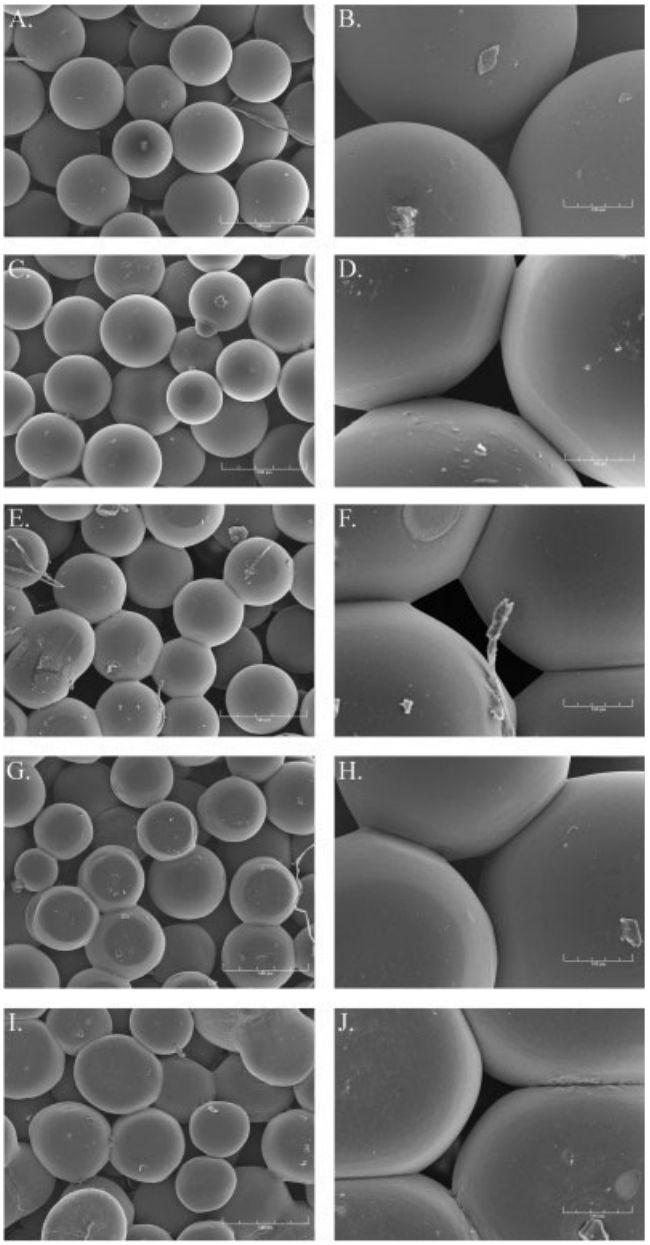

Figure 4. Effect of submersion time on the resulting morphology of the sintered microsphere scaffold. Higher submersion times resulted in small increases in the bonding between microspheres. After a submersion time of 10 min, the microspheres start to lose their spherical morphology. The 50× and 200× SEM images of PLAGA scaffolds with varying submersion time points while maintaining the sintering solution concentration at 20% (vol/vol) acetone/ethanol: A. 0 min 50×, B. 0 min. 200×, C. 1 min. 50×, D. 1 min. 200×, E. 5 min. 50×, F. 5 min. 200×, G. 10 min. 50×, H. 10 min. 200×, I. 30 min. 50×, J. 30 min. 200×.

is an SEM of the nine scaffolds analyzed and illustrates a clear change in scaffold morphology with an increase in sintering solution concentration for both the PNEA and PNEPhA, Figure 8 (A–C) and (G–I), respectively. The PNMV microsphere scaffolds were found to have a 33.1% ± 1.3% porosity for the low sintering solution, 36.0% ± 1.7% for the mid sintering solution and 37.6% ± 0.8%

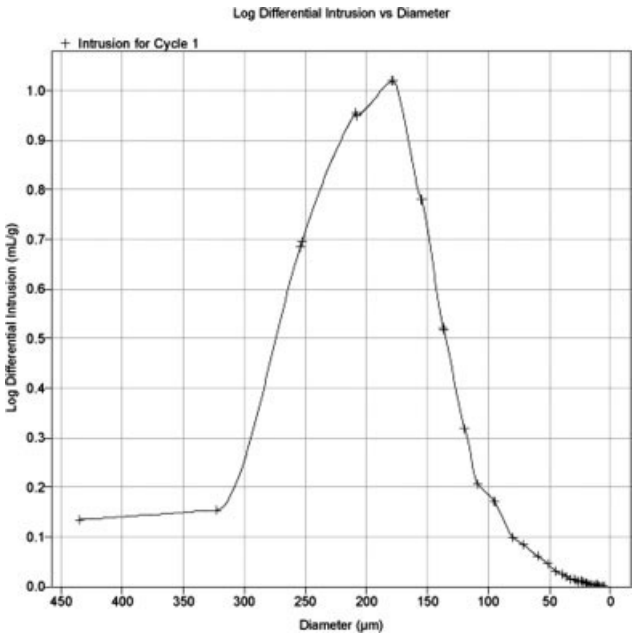

Figure 5. Distribution of pore sizes in PLAGA scaffolds created using a 20% acetone/ethanol solvent/non-solvent sintering solution.

porosity for the high sintering solution. The porosities found for the PNMV microsphere scaffolds were found to have the opposite trend and had a significantly higher porosity for the high concentration compared with the low concentration. Figure 8 (D–F) depicts the resulting PNMV scaffolds at each sintering solution and clearly illustrates a large amount of microsphere debris from fractured microspheres. The average pore diameters for PNEA microsphere scaffolds are: 120.4 ± 8.6 μm for the low sintering solution, 100.6 ± 8.5 μm for the mid sintering solution and 103.0 ± 4.4 μm for the high sintering solution. The PNMV scaffold average pore diameters are: 104.0 ± 0.9 μm for the low sintering solution, 78.6 ± 3.7 μm for the mid sintering solution and 80.1 ± 1.9 μm for the high sintering

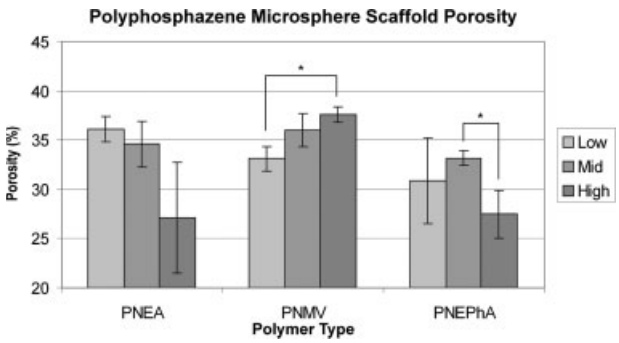

Figure 6. Effect of solvent concentration on the interconnected porosity of sintered microsphere scaffolds composed of PNEA, PNMV and PNEPhA. Statistical significance tested between the three sintering solution concentrations for each polymer, and found between the low and high PNMV scaffolds and also between the mid and high PNEPhA scaffolds. * represents statistical significance with $p < 0.05$.

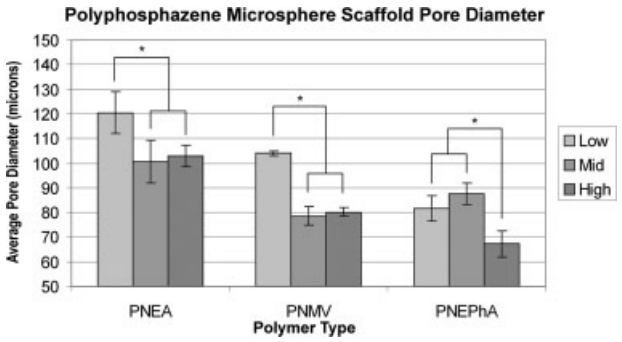

Figure 7. Effect of solvent concentration on the average pore diameter of sintered microsphere scaffolds composed of PNEA, PNMV, and PNEPhA. Statistical significance tested between the three sintering solution concentrations for each polymer, and found between: the low and mid PNEA scaffolds, the low and high PNEA scaffolds, the low and mid PNMV scaffolds, the low and high PNMV scaffolds, the low and high PNEPhA scaffolds and the mid and high PNEPhA scaffolds. * represents statistical significance with $p < 0.05$.

solution. The PNEPhA scaffold average pore diameters are: 81.7 ± 5.1 μm for the low sintering solution, 87.5 ± 4.2 μm for the mid sintering solution and 67.2 ± 5.4 μm for the high sintering solution. The average pore diameters are depicted in Figure 7 and illustrate a significant difference between the low sintering solution concentration when compared with either the mid or high sintering solution concentration for the PNEA and PNMV microspheres. The PNEPhA microspheres illustrate a significant difference between the low and mid sintering solution concentration when compared with the high sintering solution concentration. For all three polyphosphazenes tested there is a threshold sintering solution concentration that when crossed results in approximately a 20 μm decrease in average pore diameter.

Polyphosphazene Scaffold Compression Testing

The PNMV and PNEPhA scaffolds were tested to determine their individual compressive moduli. These results are depicted in Figure 9 and illustrate a decreasing trend in modulus for PNMV microspheres starting at 24.2 MPa for the low sintering solution and falling to 16.1 MPa for the mid and 13.1 MPa for the high sintering solution. There is no statistical significance for the PNMV moduli. The

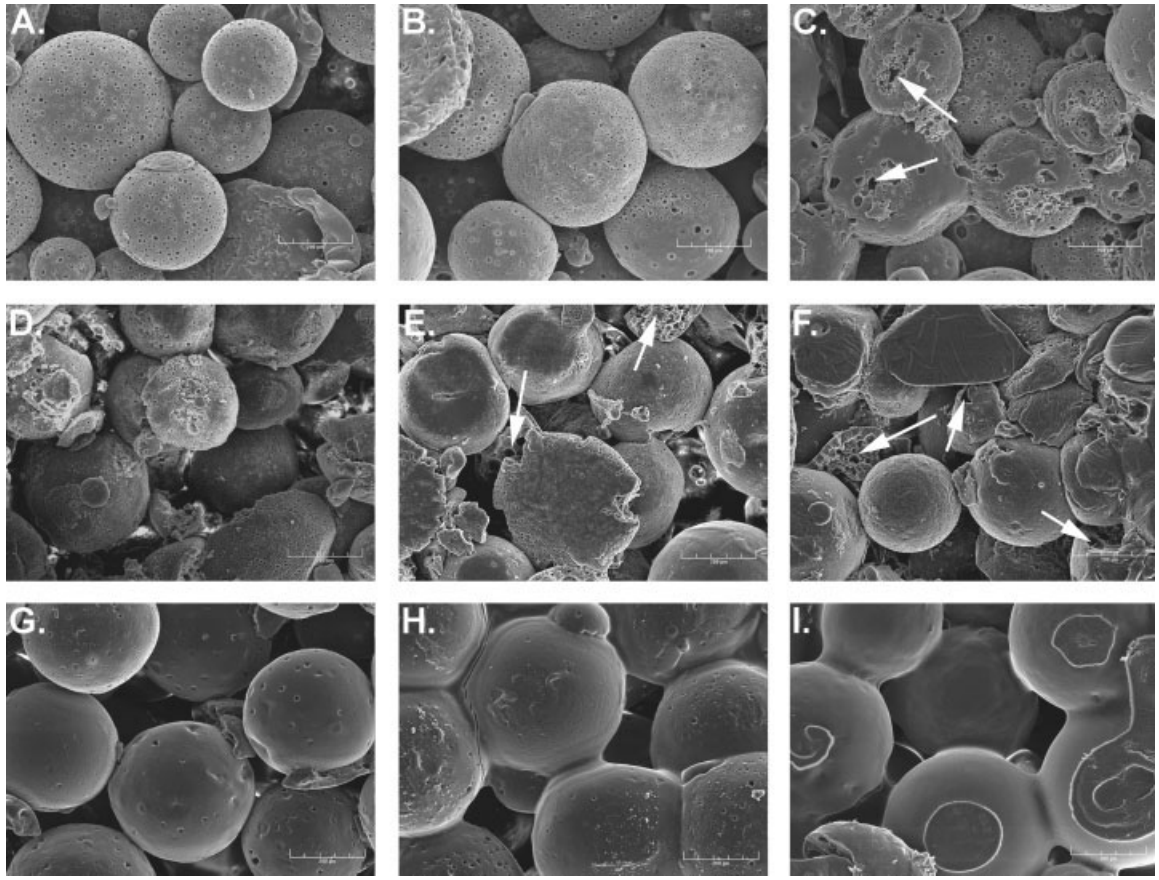

Figure 8. Effect of sintering solution concentration on resulting morphology of lighter than water microsphere scaffolds composed of PNEA, PNMV, and PNEPhA. Arrows indicate where the high solvent levels caused partial erosion of the microspheres and exposure of the porous interior of the individual microspheres. A. PNEA with low sintering solution, B. PNEA with mid sintering solution, C. PNEA with high sintering solution, D. PNMV with low sintering solution, E. PNMV with mid sintering solution, F. PNMV with high sintering solution, G. PNEPhA with low sintering solution, H. PNEPhA with mid sintering solution, I. PNEPhA with high sintering solution.

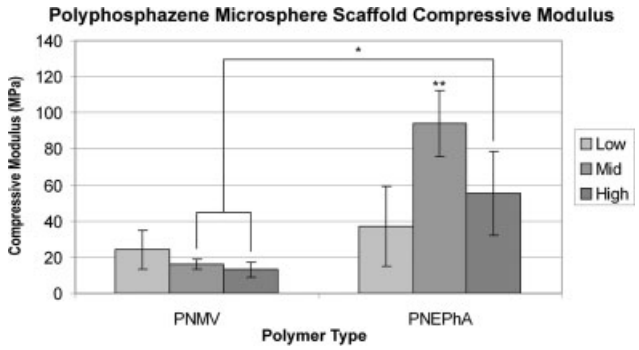

Figure 9. Effect of sintering solution concentration on the compressive modulus of lighter than water microsphere scaffolds composed of PNMV and PNEPhA. PNEA was excluded from the compressive testing because it exists in a plastic state at room temperature. Statistical significance tested between all of the moduli reported. * represents statistical significance with $p < 0.05$ for moduli indicated. ** represents statistical significance with $p < 0.05$ between the indicated modulus and all other moduli reported.

PNEPhA microsphere scaffold moduli exhibited a rise and fall as the sintering solution concentration increased. The low sintering solution produced a modulus of 36.5 MPa, the mid solution produced a modulus of 94.3 MPa and the high sintering solution produced a modulus of 55.3 MPa. The PNEPhA mid sintering solution modulus was statistically significant from all other polymer sintering solution combinations and the PNEPhA high sintering solution modulus was statistically significant when compared with the mid and high PNMV scaffolds.

DISCUSSION

Solvent/non-solvent sintering effectively sinters a range of different polymers based on Flory–Huggins solution theory, which states that a greater affinity between the solvent and polymer will allow the solvent to dissolve progressively longer chains of the polymer.[17] This concept is the reason why Figure 2 illustrates an increase in the bonding region between adjacent microspheres. The increase in solvent concentration allows progressively longer chains on the surface of the microspheres to swell and intertwine with each other. The sintering is completed when the more volatile solvent begins to evaporate at a greater rate than the less volatile non-solvent, which decreases the affinity of solvent/non-solvent mixture for the surface chains and causes polymer precipitation resulting in bonding between the microspheres.[17] If the solvent concentration becomes too high, dissolution will occur freeing the smaller surface chains and leading to the occlusion of the pores and flattening of the resulting scaffold as observed for PLAGA microspheres sintered with a 40% (vol/vol) acetone/ethanol solvent/non-solvent sintering solution in Figure 2 (I,J). At solvent compositions less than 40% (vol/vol) acetone/ethanol dissolution does not occur and instead the composition determines the extent of the sintering. The solvent/non-solvent sintering solution composition exhibited the same correlation on the bonding region for PNEA, PNMV and PNEPhA sintered microspheres as it did for PLAGA. This verifies the versatility of the technique to have control over the degree of sintering across a range of polymers.

The length of time the microspheres are submerged in the solvent/non-solvent sintering solution before they are molded appears to affect the bonding region only slightly and has a more profound effect on the morphology of the microspheres. Presumably the slight correlation between submersion time and bonding region is caused by quickly reaching a steady state between the solvent/non-solvent sintering solution and the microsphere surface. The long submersion time allows diffusion of the sintering solution throughout the microsphere allowing interior polymer chains to move in relation to each other resulting in a change in the spherical morphology of the microsphere.[17,23]

Microsphere scaffolds fabricated from PLAGA, PNEA, PNMV, and PNEPhA all exhibited porosities similar to those observed with heat sintered microspheres[1] and produced average pore diameters that are in the range necessary for *in vitro* cell culture as well as *in vivo* scaffold implantation.[18,24] These results verify the ability of solvent/non-solvent sintering to retain an open porosity throughout the volume of the microsphere scaffold, which is a crucial design characteristic for tissue engineering constructs.[25] Additionally the porosities and pore diameters of the PNEA and PNEPhA scaffolds showed a significant dependence on the solvent/non-solvent sintering solution composition with the overall trend being a decrease in porosity and pore diameter at high compositions as evidenced by Figures 7 and 9. This is an expected relationship based on the Flory–Huggins solution theory as the higher solvent compositions create a greater bonding region which occludes some of the porosity while decreasing the diameter of the resulting pore. The PNMV had the opposite trend with respect to the total porosity, which is thought to be caused by an exposure of the interior porosity of the microspheres due to fracturing or dissolution of the surface chains covering the interior pores. The fracturing of the PNMV microspheres is clearly evident in Figure 8 (D–F) which illustrates a large amount of irregular debris. This debris could also contribute to the observed trend in porosity due to inefficient packing of the microspheres, however it would be expected that the debris would be present at all concentrations and would thus not support the significant increase found in total interconnected porosity for PNMV scaffolds at high solvent compositions. This leads to the more likely conclusion that the increased porosity found with PNMV is due to dissolution of the individual microsphere surface covering the interior pores or partial erosion of the hollow microspheres which would additionally result in the irregular shaped debris indicated by arrows of Figure 8 (E,F). The exposure of interior pores due to dissolution of the

surface covering the pores is also seen to a small degree with the PNEA scaffolds at the high solvent composition in Figure 8 (C). Exposure of the interior pores of the PNMV would result in both an increase in total interconnected porosity and a decrease in the pore size which would support the findings reported in Figures 7 and 9.

Finally the compressive modulus of the PNEPhA scaffolds showed a significant correlation with solvent/non-solvent sintering solution composition. The highest modulus observed was found at the middle concentration. The increase in modulus from the low to mid is expected as the bonding region should be greater, and consequently less likely to fracture at the mid concentration. However, the decrease in modulus from the mid to the high composition is somewhat unexpected. This decrease can be attributed to dissolution of the surface chains on the porous PNEPhA scaffolds resulting in a loss of integrity of the individual microspheres leading to premature fracture of the individual microspheres as opposed to fracture of the bonding region between the spheres. The loss of microsphere integrity could occur when the shell of a hollow microsphere is thinned by the solvent/non-solvent sintering solution. The resulting thin shelled microsphere is then more susceptible to failure. Figure 9 (I) supports the claim that there is surface chain dissolution by providing visual evidence that there was an accumulation of dissolved polymer creating flat spots at the bottom of several microspheres. The mechanical properties of PNMV microspheres showed no dependence on solvent/non-solvent sintering solution composition, which suggests the observed modulus corresponded with the bulk material or the individual microsphere and not the bonding region between the microspheres.

CONCLUSIONS

The solvent/non-solvent sintering technique provides a quick, reproducible, mild, and flexible means for creating porous interconnected structures as scaffolds for tissue engineering, drug delivery, filtration or any other application where polymer surfaces need to be sintered. It can be used regardless of the glass transition temperature of a polymer, and can be tailored to produce the desired degree of microsphere interconnectivity by varying the concentration of the solvent/non-solvent sintering solution, and to a lesser extent by varying the submersion time in the sintering solution. Microspheres do not dissolve in the sintering solution after extended periods of time and still illustrate a predictable degree of sintering. In addition the solvent/non-solvent sintering technique produces a median pore size and porosity similar to the heat sintered microspheres. Solvent/non-solvent sintering effectively produced lighter than water polyphosphazene microsphere scaffolds with PNEPhA microsphere scaffolds sintered with the mid sintering solution concentration exhibiting the best combination of mechanical strength and porosity. Being a much milder method, the solvent/non-solvent sintering technique could potentially allow preloading of bioactive factors within the scaffold for controlled/sustained release. The solvent/non-solvent sintering technique does not require a specific mold geometry since heat transfer is not an issue, thereby enabling an infinite number of final microsphere scaffold geometries. This technique potentially allows for the creation of a final scaffold geometry custom tailored to the needs of the patient.

REFERENCES

1. Borden M, Attawia M, Khan Y, Laurencin CT. Tissue engineered microsphere-based matrices for bone repair: Design and evaluation. Biomaterials 2002;23:551–559.
2. Borden M, Attawia M, Laurencin CT. The sintered microsphere matrix for bone tissue engineering: *In vitro* osteoconductivity studies. J Biomed Mater Res 2002;61:421–429.
3. Laurencin CT, Borden M. Methods for using microsphere polymers in bone replacement matrixes and composition produced thereby. US Patent 5,866,155; 1999.
4. Fleming JE Jr, Cornell CN, Muschler GF. Bone cells and matrices in orthopedic tissue engineering. Orthop Clin North Am 2000;31:357–374.
5. Yu X, Botchwey EA, Levine EM, Pollack SR, Laurencin CT. Bioreactor-based bone tissue engineering: The influence of dynamic flow on osteoblast phenotypic expression and matrix mineralization. Proc Natl Acad Sci USA 2004;101:11203–11208.
6. Jang JH, Shea LD. Controllable delivery of non-viral DNA from porous scaffolds. J Control Release 2003;86:157–168.
7. Borden M, Attawia M, Khan Y, El-Amin SF, Laurencin CT. Tissue-engineered bone formation *in vivo* using a novel sintered polymeric microsphere matrix. J Bone Joint Surg Br 2004;86:1200–1208.
8. Borden M, El-Amin SF, Attawia M, Laurencin CT. Structural and human cellular assessment of a novel microsphere-based tissue engineered scaffold for bone repair. Biomaterials 2003;24:597–609.
9. Khan YM, Katti DS, Laurencin CT. Novel polymer-synthesized ceramic composite-based system for bone repair: An *in vitro* evaluation. J Biomed Mater Res A 2004;69:728–737.
10. Bellehumeur CT, Bisaria MK, Vlachopoulos J. An experimental study and model assessment of polymer sintering. Polym Eng Sci 1996;36:2198–2207.
11. Allcock HR. Chemistry and Applications of Polyphosphazenes. New York: Wiley; 2003.
12. Allcock HR, Pucher SR, Scopelianos AG. Poly[(amino acid ester)phosphazenes]: Synthesis, crystallinity, and hydrolytic sensitivity in solution and the solid state. Macromolecules 1994;27:1071–1075.
13. Sethuraman S. Low Temperature Setting Polymer-Ceramic Composites for Bone Tissue Engineering. Philadelphia: Drexel University; 2005. p 353.
14. Kumbar SG, Bhattacharyya S, Nukavarapu SP, Khan YM, Nair LS, Laurencin CT. In vitro and *in vivo* characterization of biodegradable poly(organophosphazenes) for biomedical applications. J Inorg Organometallic Polym Mater 2006;16:365–385.
15. Kumbar SG, Nair LS, Bhattacharyya S, Laurencin CT. Polymeric nanofibers as novel carriers for the delivery of therapeutic molecules. J Nanosci Nanotechnol 2006;6:2591–2607.
16. Laurencin CT, El-Amin SF, Ibim SE, Willoughby DA, Attawia M, Allcock HR, Ambrosio AA. A highly porous 3-dimen-

sional polyphosphazene polymer matrix for skeletal tissue regeneration. J Biomed Mater Res 1996;30:133–138.
17. Ebewele RO. Polymer Science and Technology, Vol. 544. New York: CRC Press; 1998. p 316–326.
18. Akay G, Birch MA, Bokhari MA. Microcellular polyHIPE polymer supports osteoblast growth and bone formation *in vitro*. Biomaterials 2004;25:3991–4000.
19. Singh A, Krogman NR, Sethuraman S, Nair LS, Sturgeon JL, Brown PW, Laurencin CT, Allcock HR. Effect of side group chemistry on the properties of biodegradable L-alanine co-substituted polyphosphazenes. Biomacromolecules 2006;7: 914–918.
20. Park PIP, Jonnalagadda S. Predictors of glass transition in the biodegradable polylactide and poly-lactide-*co*-glycolide polymers. J Appl Polym Sci 2006;100:1983–1987.
21. Phenix A. Solubility parameters and the cleaning of paintings: An update and review. Kunsttechnologie und Konservierung 1998;12:397–409.
22. Phenix A, Sutherland K. The cleaning of paintings: Effects of organic solvents on oil paints films. Rev Conservation 2001;2: 47–60.
23. Vrentas JS, Vrentas CM. Solvent self-diffusion in rubbery polymer-solvent systems. Macromolecules 1994;27:4684–4690.
24. Karageorgiou V, Kaplan D. Porosity of 3D biomaterial scaffolds and osteogenesis. Biomaterials 2005;26:5474–5491.
25. Rezwan K, Chen QZ, Blaker JJ, Boccaccini AR. Biodegradable and bioactive porous polymer/inorganic composite scaffolds for bone tissue engineering. Biomaterials 2006;27:3413–3431.